Available online at www.sciencedirect.com

ScienceDirect

Geochimica et Cosmochimica Acta 283 (2020) 54–66

Geochimica et Cosmochimica Acta

www.elsevier.com/locate/gca

Mg/Ca-Temperature Calibration of Polar Benthic foraminifera species for reconstruction of bottom water temperatures on the Antarctic shelf

Elaine M. Mawbey [a,*], Katharine R. Hendry [b], Mervyn J. Greaves [c], Claus-Dieter Hillenbrand [a], Gerhard Kuhn [d], Charlotte L. Spencer-Jones [e], Erin L. McClymont [e], Kara J. Vadman [f], Amelia E. Shevenell [f], Patrycja E. Jernas [g], James A. Smith [a]

[a] *British Antarctic Survey, High Cross, Madingley Road, Cambridge CB3 0ET, UK*
[b] *School of Earth Sciences, Faculty of Science, University of Bristol, Wills Memorial Building Queen's Road, Bristol BS8 1RJ, UK*
[c] *The Godwin Laboratory for Palaeoclimate Research, Department of Earth Sciences, University of Cambridge, Downing St., Cambridge CB2 3EQ, UK*
[d] *Alfred-Wegener-Institut Helmholtz-Zentrum für Polar- und Meeresforschung, Am Alten Hafen 26, 27568 Bremerhaven, Germany*
[e] *Department of Geography, Durham University, Durham DH 1 3LE, UK*
[f] *College of Marine Science, University of South Florida, St. Petersburg, FL, USA*
[g] *Department of Marine Geology, Institute of Oceanography, University of Gdańsk, Aleja Marszałka Józefa Piłsudskiego 46, 81-378 Gdynia, Poland*

Received 2 August 2019; accepted in revised form 23 May 2020; Available online 4 June 2020

Abstract

Benthic foraminifera Mg/Ca is a well-established bottom water temperature (BWT) proxy used in paleoclimate studies. The relationship between Mg/Ca and BWT for numerous species has been determined using core-top and culturing studies. However, the scarcity of calcareous microfossils in Antarctic shelf sediments and poorly defined calibrations at low temperatures has limited the use of the foraminiferal Mg/Ca paleothermometer in ice proximal Antarctic sediments. Here we present paired ocean temperature and modern benthic foraminifera Mg/Ca data for three species, *Trifarina angulosa*, *Bulimina aculeata*, and *Globocassidulina subglobosa,* but with a particular focus on *Trifarina angulosa.* The core-top data from several Antarctic sectors span a BWT range of −1.7 to +1.2 °C and constrain the relationship between Mg/Ca and cold temperatures. We compare our results to published lower-latitude core-top data for species in the same or related genera, and in the case of *Trifarina angulosa,* produce a regional calibration. The resulting regional equation for *Trifarina angulosa* is Temperature (°C) = (Mg/Ca −1.14 ± 0.035)/0.069 ± 0.033). Addition of our *Trifarina angulosa* data to the previously published *Uvigerina spp.* dataset provides an alternative global calibration, although some data points appear to be offset from this relationship and are discussed. Mg-temperature relationships for *Bulimina aculeata* and *Globocassidulina subglobosa* are also combined with previously published data to produce calibration equations of Temperature (°C) = (Mg/Ca-1.04 ± 0.07)/0.099 ± 0.01 and Temperature (°C) = (Mg/Ca-0.99 ± 0.03)/0.087 ± 0.01, respectively. These refined calibrations highlight the potential utility

* Corresponding author.
E-mail address: elawbe@bas.ac.uk (E.M. Mawbey).

https://doi.org/10.1016/j.gca.2020.05.027
0016-7037/

of benthic foraminifera Mg/Ca-paleothermometry for reconstructing past BWT in Antarctic margin settings.

Keywords: Mg/Ca-temperature calibration; Benthic foraminifera; Antarctica; Paleotemperature reconstruction; Core-tops

1. INTRODUCTION

Satellite observations indicate that the West Antarctic Ice Sheet (WAIS) is losing mass at an accelerating rate (Rignot et al., 2019). Mass loss is primarily driven by basal melting of ice shelves by warm Circumpolar Deep Water (CDW), which upwells at the continental shelf edge and moves across the shelf through bathymetric troughs to grounding lines (Pritchard et al., 2012). CDW is characterised by temperatures >3.5 °C above in-situ freezing point and salinities >34.6 and tends to flow onto the shelf at depths >300 m (Jacobs et al., 2011). Ice-shelf thinning reduces buttressing of inland ice and results in flow acceleration, drawdown of the interior ice sheet (Pritchard et al., 2012), and sea-level rise (Edwards et al., 2019).

Of particular concern is the future behaviour of ice streams draining into the Amundsen Sea Embayment (ASE), such as Pine Island and Thwaites glaciers, which contain ~1.4 m of sea level-equivalent ice (Vaughan et al., 2006). Accurately predicting the future response of glaciers in this region to ongoing warming (e.g., DeConto and Pollard, 2016) requires a comprehensive understanding of the potential influence of CDW on Antarctic glaciers over coming decades and centuries (Colleoni et al., 2018). Recent work suggests that the flux of CDW is controlled by the strength and intensity of westerly winds at the shelf edge (Jenkins et al., 2018) which in turn is driven by tropical climate dynamics (Steig et al., 2012; Dutrieux et al., 2014; Jenkins et al., 2018; Holland et al., 2019). Indeed, sediment cores recovered from beneath the floating part of Pine Island Glacier indicate that it started to retreat in the 1940 s (Smith et al., 2017), possibly as a response to prolonged El Niño conditions (Steig et al., 2012). Furthermore, Dutrieux et al. (2014) demonstrated that oceanic melting of Pine Island Glacier decreased by 50% between 2011 and 2012 due to a strong La Niña event, which weakened the typically cyclonic wind stress and curtailed the westerlies. With the realisation that CDW forcing might change on a variety of timescales from decades (Jenkins et al., 2018) to centuries (Hillenbrand et al., 2017), there is a growing need to reconstruct its presence/absence over Antarctica's continental shelves over a range of timescales. However, because regional physical oceanographic data are limited to the last two decades, it is unclear whether the CDW has been a persistent feature on the ASE shelf, or if the advection and/or temperature of CDW on the shelf has varied in the past. To provide context for recent observations and improve understanding of the future behaviour of ice sheets in Antarctica, detailed records of past seawater temperatures are required from Antarctica's continental shelves (Shevenell et al., 2011; Hillenbrand et al., 2017).

Previous attempts to reconstruct CDW advection onto the Antarctic shelf utilised a range of proxies that are related to seawater temperatures, such as diatom and foraminifera assemblages (Leventer et al., 2002; Peck et al., 2015; Minzoni et al., 2017; Majewski et al., 2017; Hillenbrand et al., 2017) and stable oxygen and carbon isotopes of both planktic and benthic foraminifera tests (Shevenell and Kennett, 2002; Peck et al., 2015; Hillenbrand et al., 2017). However, each of these proxies has its own limitations. For example, stable oxygen isotope ($\delta^{18}O$) in foraminifera vary with both temperature and $\delta^{18}O$ seawater, which proximal to Antarctica is influenced primarily by ice volume and glacial meltwater (Shackleton, 1967; Meredith et al., 2008), whereas stable carbon isotopes are influenced by biological productivity and water mass nutrient concentration (see references in Hillenbrand et al., 2017). Furthermore, despite some successes reconstructing upper ocean temperatures on the Antarctic shelf using biomarkers (TEX_{86}; Shevenell et al., 2011; Kim et al., 2012; Etourneau et al., 2013), only a single study in Prydz Bay, East Antarctica, attempted to reconstruct BWT on the Antarctic shelf (Rathburn and De Deckker, 1997). Consequently there is a dearth of information on past BWT from ice proximal settings around Antarctica, where these records are urgently needed.

Benthic foraminifera Mg/Ca paleothermometery potentially offers a powerful tool for reconstructing past temperatures in ice-proximal settings around Antarctica. Mg/Ca-temperature calibrations have been developed for different benthic foraminifera species (e.g. Rosenthal et al., 1997; Elderfield et al., 2006; Marchitto et al., 2007; Bryan et al., 2008; Evans et al 2015) in a wide range of environments (Barrientos et al., 2018). However, there is a distinct lack of core-top calibration data for low temperature polar environments. Low temperature Mg/Ca calibrations from the Arctic and Antarctic for common high-latitude benthic foraminifer species (e.g., *Trifarina angulosa, Globocassidulina subglobosa* and *Bulimina aculeata)* are therefore urgently required to facilitate the interpretation of down-core benthic Mg/Ca records from the polar-regions. The lack of Mg/Ca calibration data from Antarctica stems from two fundamental issues: First, calcareous foraminifera are often either poorly preserved or not abundant in many shelf regions around Antarctica. Second, the number of sites where both BWTs were directly measured by CTD casts and where surface sediments were collected is limited.

To address this data gap, we generated Mg/Ca temperature data from three species of benthic foraminifera occupying a range of BWT around Antarctica: *Trifarina angulosa, Globocassidulina subglobosa,* and *Bulimina aculeata* (Fig. 1). However, we focus primarily on the species *Trifarina angulosa* for the following reasons: (1) it is common in modern and Holocene sediments on the Antarctic continental shelf, and particularly in our main study area in the Amundsen Sea (e.g., Hillenbrand et al., 2017;

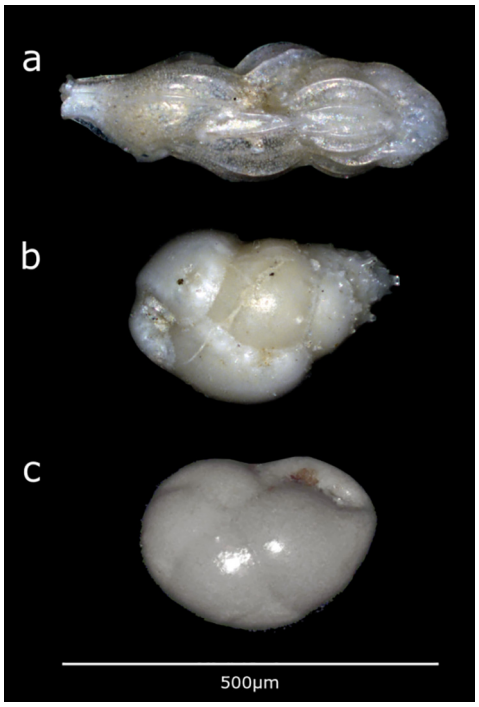

Fig. 1. Stacked light microscope images of a) *Trifarina angulosa,* b) *Bulimina aculeata;* umbilical view, and c). *Globocassidulina subglobosa;* umbilical view.

Majewski et al., 2017); (2) it is a shallow infaunal species (Mackensen et al., 1990), which is genetically related to *Uvigerina* spp., with *Uvigerina peregrina* being more closely related to *Trifarina angulosa* (*Trifarina earlandi*) than to some other *Uvigerina* species (Schweizer et al. 2005, Schweizer et al., 2011). Published Mg/Ca-temperature calibrations were produced for *Uvigerina* spp. (summarised in Elderfield et al., 2010), to which we can compare our *Trifarina angulosa* records; and (3) shallow infaunal species are less likely to be influenced by the effects of carbonate ion concentration on the Mg/Ca ratios of their tests than epifaunal species (Elderfield et al., 2010). Changes in carbonate ion saturation state are known to have a secondary effect on Mg/Ca values in some foraminifera (e.g. Elderfield et al., 2006, Bryan and Marchitto, 2008).

However, changes in environmental conditions over time may lead to considerable changes in the down-core abundance or presence of certain foraminifera species, implying that continuous down-core records are difficult to obtain (Hillenbrand et al., 2017). Therefore, we also investigate two other calcareous benthic foraminifera that are common on the Antarctic shelf: *Globocassidulina subglobosa* and *Bulimina aculeata*.

Globocassidulina subglobosa is an important species that is common on the West Antarctic continental shelf, for example both on the West and the East side of the Antarctic Peninsula (Majewski and Pawlowski, 2010) and in the Amundsen Sea (Majewski, 2013; Hillenbrand et al., 2017). The species has been shown to dominate biofacies in fjords on the western Antarctic Peninsula (Ishman, 1990) and is sometimes associated with ice-proximal settings (Majewski and Anderson, 2009) and sub-ice-shelf settings (Murray and Pudsey, 2004). Live *Globocassidulina subglobosa* have been found at 0–1 cm depth in the sediments and, thus, can be considered as shallow infaunal (Murray and Pudsey, 2004).

Bulimina spp. Mg/Ca has recently been calibrated to BWT over a wide temperature range (3-13 °C), but not one that includes typical Antarctic margin BWTs of ~−1 to +2 °C (Grunert et al., 2018). On Antarctica's continental shelves, *Bulimina aculeata* has been associated with nutrient-rich, muddy sediments associated with quiescent CDW-dominated environments (Ishman and Domack, 1994; Shevenell and Kennett, 2002; Majewski, 2013). As such, Mg/Ca-temperature data from this species may be the most useful for determining past variations in the advection of CDW onto the Antarctic continental shelf. *Bulimina aculeata* is thought to be shallow infaunal and occurrs in the uppermost 0–1 cm of the seabed sediments (Mackensen et al., 1990).

By examining the Mg/Ca-temperature relationship for these three species, we hope to assess the utility of this proxy in Antarctic ice-proximal settings, and ultimately, enable future studies to reconstruct past BWT in climatically sensitive regions such as the Amundsen Sea.

2. MATERIALS AND METHODS

2.1. Sample site locations and collection

We selected samples from several locations in different sectors around Antarctica (Fig. 2) to encompass a range of BWTs from –1.75 °C to + 1.23 °C. Samples from the eastern Pacific sector span the warm water regime (CDW), whilst the samples from the East Antarctic shelf in the Weddell Sea and on the Sabrina Coast (close to Totten Glacier) span the colder water regime. This sampling strategy achieves the widest temperature range for calibration as possible with available material.

The samples (Table 1) can be geographically categorised into five continental shelf regions: the Amundsen Sea, Bellingshausen Sea, western Antarctic Peninsula, Weddell Sea, and the Sabrina Coast. All samples were taken by box core except the Sabrina Coast samples, which were recovered with a large volume multiple-corer. This strategy assures that benthic foraminifera tests were collected from undisturbed seafloor surface sediments and are most likely of modern age. In contrast, foraminifera specimens taken from piston, gravity or kasten core tops are sometimes of older age due to core-top disturbance and/or seafloor surface sediment loss during core recovery. The samples span a water depth range of 61–1789 m but most sites (with the exception of two) are shallower than 715 m (Table 1).

All our samples were processed in a similar way, with the exception that the foraminifera from the eastern Weddell Sea and the Sabrina Coast were Rose Bengal stained; their stained protoplasm indicates that the individuals were alive/recently dead at the time of sampling. The surface sediment samples were washed with deionised water through a 63 µm sieve and dried for 24 hours at 40 °C in an oven; the Sabrina Coast samples were washed on the ship, 24 hours

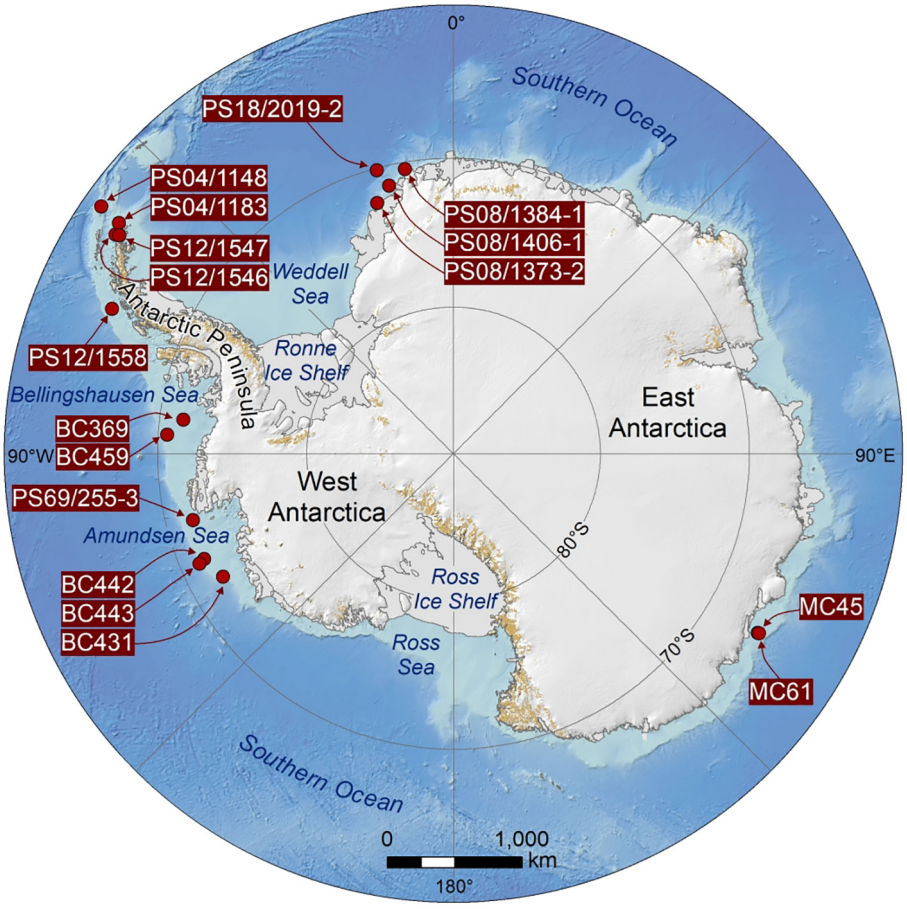

Fig. 2. Sample site locations around Antarctica.

after collection and staining. The >63 μm fraction was dry-sieved and specimens of *Trifarina angulosa*, *Bulimina aculeata,* and *Globocassidulina subglobosa* were picked from the 250–355 μm fraction, where possible (approximately 30 specimens per sample), except for the Sabrina Coast samples, which were picked from the 150–355 μm size fraction due to low total foraminifer abundance. The potential influence of test size was assessed for *Trifarina angulosa* by picking tests from the 150–250 μm fraction and comparing their Mg/Ca ratios to those of tests from the 250–355 μm fraction. All specimens of *Trifarina angulosa* were the Costate (ribbed) morphotype (Fig. 1a), except for the Sabrina Coast samples, which also included the "Hispid" (spiky) morphotype. This was again necessary to obtain enough material for analysis.

For some samples, the BWT at the same site was measured by a CTD cast deployed at the same time (Table 1). However, for other sites no concurrent CTD profiles were available. To determine BWTs for these sites, the temperature at the same water depth from the nearest available CTD cast was used. The CTD data used and distance from the sample site are given in Table 1. The CTD data were collected in austral spring/summer, which most likely is also the main period when the foraminifera would be calcifying due to increase in food supply and reduction in sea-ice cover (Mackensen et al., 1993, Skirbekk et al., 2016).

2.2. Foraminifera cleaning and analysis

Foraminifera specimens were gently crushed between two glass plates and visible contaminants were removed using a fine paintbrush. The fragments then underwent a cleaning procedure adapted from Boyle and Keigwin (1985/86). This includes: (i) the removal of clay by ultrasonication of test fragments 3x in 18.2 MΩ·cm deionised water and 3x in methanol; (ii) a reductive step to remove any metal oxides using a solution of hydrous hydrazine and citric acid in ammonia; (iii) an oxidative step using a solution of hydrogen peroxide in sodium hydroxide to remove organic matter; and (iv) a dilute nitric acid leach using Optima pure nitric acid. Between the mechanical clay removal step and the reductive step, samples were examined under a binocular microscope and any obvious non-carbonate particles removed. The cleaned samples were dissolved in ultra-pure nitric acid (0.1 M HNO_3), centrifuged, and a 'concentrate' aliquot was transferred to a new sample vial to prevent leaching from any remaining contaminants. This aliquot was then split for analysis by ICP-OES and HR-ICP-MS. This was done so that we could follow the method of Misra et al. (2014), using the HR-ICP-MS to quantify B/Ca at low concentrations. All other trace metal data is from analysis by ICP-OES following the method of de Villiers et al. (2002). Long-term instrumental precision of

Table 1
Core ID, cruise, location and bottom-water temperature (BWT) information for each sample, size fraction analysed and Mg/Ca data for each species.

Core ID	Cruise	Lati	Long	Water depth (m)	BWT (°C)	CTD/data source	CTD distance from core site (km)	depth CTD measurement from (m)	Shellsize fraction (μm)	Sample depth (cm)	Mg/Ca (mmol/mol)		
											T.angulosa	*C.subglobosa*	*B.aculeata*
PS08/1373–2	ANT-1V/3	−72.25	−16.88	1237	0.32	taken at time of sample	0	1237	150–250	0–2	1.190	-	-
									250–355		1.318		
PS08/1384–1	ANT-1V/3	−70.47	−9.62	714	−0.97	taken at time of sample	0	714	150–250	0–2	0.987	-	-
									250–355		1.122		
PS08/1406–1	ANT-1V/3	−71.33	−13.42	237	−1.75	taken at time of sample	0	237	150–250	0–2	1.158	-	-
									250–355		0.954		
PS18/2019–2	ANT-1X/3	−70.15	−15.10	161	−1.5	taken at time of sample	0	161	150–250	0–2	1.066	-	-
									250–355		1.043		
BC369	JR104	−71.58	−82.86	587	1.23	JCR141 CTD 029	163	587	150–250	0–1	1.124	-	
									250–355		1.206		1.285
BC431	JR141	−72.30	−118.16	512	0.15	JCR141 CTD 019	0	498	150–250	0–1	0.983	-	
									250–355		1.046		-
BC442	JR141	−71.68	−113.01	608	0.92	JCR141 CTD 025	12	606	150–250	0–1	1.191	-	
									250–355		1.150		1.200
BC443	JR141	−71.28	−113.46	1789	0.67	JCR 84 CTD 011	8	1789	150–250	0–1	1.354	-	
									250–355		1.377		-
BC459	JR141	−70.61	−86.25	676	1.01	JCR141 CTD 029	0	656	150–250	0–1	1.136	-	
									250–355		1.194		1.428
PS69/255–3	ANT-XXIII/4	−71.80	−104.36	654	1.07	Geotracers NBP0901 CTD 007	47	654	150–250	0–1	1.059	-	
									250–355		1.092		1.36
MC45	NBP14–02	−66.19	120.50	546	0.3	taken at time of sample	0	546	150–355	0–1	0.936	-	-
MC61	NBP14–02	−66.13	120.46	580	0.5	taken at time of sample	0	580	150–355	0.5–3.5	0.881	-	-
PS12/1546	ANT-VI/2	−63.00	−57.00	67	−1.45	PS12/132–1	0	71	250–355	1–1.5	-	0.921	-
PS12/1558	ANT-VI/2	−65.07	−66.98	200	1.12	Schmidtko et al., 2014	n/a	n/a	250–355	0–1	-	0.871	-
PS12/1547	ANT-VI/2	-63.24	−56.84	137	−1.61	PS12/133–1	0	140	250–355	0–1	-	0.949	-
PS04/1183	ANT-II/3	−62.78	−55.40	112	−1.00	PS04/270–1	0	100	250–355	0–1	-	0.696	-
PS04/1148	ANT-II/3	−61.23	54.91	61	−0.25	Schmidtko et al., 2014	n/a	n/a	250–355	0–1	-	0.842	-

element ratio data determined by replicate analyses of a consistency standard prepared at Cambridge University with a magnesium/calcium ratio = 1.3 mmol mol^{-1} is ±0.55%. The accuracy of Mg/Ca determinations was established by interlaboratory comparison studies (Greaves et al., 2008; Rosenthal et al., 2004). The cleaning efficiency was monitored by measuring Mn/Ca and Fe/Ca. All samples were below the thresholds set out in Barker et al. (2003) of >0.1 mmol/mol for Mn/Ca and Fe/Ca except for one sample, which had an Fe/Ca value of 0.12 mmol/mol. The contaminant indicator trace-element/Ca ratios do not show a significant relationship with Mg/Ca (Supplementary Fig. 1), and thus no samples were eliminated from the results and discussion.

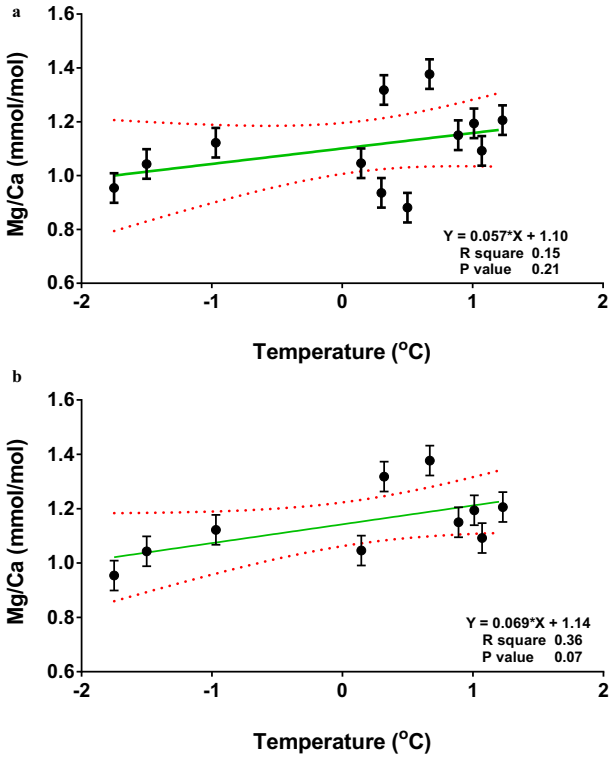

Fig. 3. Mg/Ca ratios versus temperature for *Trifarina angulosa* (a) With data from all study sites (b) without the data from the Sabrina Coast samples. Error bars are based on a repeatability study on *Uvigerina* spp. at the same analytical facilities (Elderfield et al., 2012).

3. RESULTS

3.1. *Trifarina angulosa* (250–355 μm)

Fig. 3a shows *Trifarina angulosa* Mg/Ca ratios vs. BWT for samples from the Weddell Sea, western Antarctic Peninsula, Sabrina Coast and the Bellingshausen and Amundsen seas (Table 2). We observe a weak positive linear relationship; R^2 value = 0.15, P = 0.21, number of samples = 12. The R^2 value is slightly improved if the Sabrina Coast samples are removed (R^2 = 0.36, P = 0.07, number of samples = 10). Possible reasons for this are discussed in Section 4.1.

3.1a. Trifarina Angulosa (250-355 μm)

Addition of our new dataset to the previously published *Uvigerina* spp. calibration (Elderfield et al., 2010; Bryan and Marchitto, 2008) (Fig. 4, Equations 4 and 5 (without Sabrina Coast data)) leads to a slight decrease in the R^2 value (from 0.88 to 0.83) and negligible impact on the P value (P < 0.0001) (see Table 2). Omission of the Sabrina Coast data (Equation 5) has little impact on the R^2 value (0.82) indicating that all our data fall within the variability of the *Uvigerina* spp. calibration.

3.1b. Trifarina angulosa (150–250 μm)

Supplementary Fig. 2 shows Mg/Ca ratios vs. BWT from the same sites as the 250–355 μm samples, except for Sabrina Coast, as there was insufficient material to analyse this size fraction separately. When fit to a linear regression, the 150–355 μm samples have an R^2 value of 0.08 and a P

Table 2
Compiled equations of benthic foraminiferal Mg/Ca-temperature calibrations, both previously published and from this study.

Species	Equation number	Equation $T = (Mg/Ca - c)/s$				Figure	References
		c	std error of c	s	std error of s		
Trifarina angulosa	1	1.10 ± 0.04	0.043	0.057 ± 0.043	0.043	3a	This study
Trifarina angulosa	2	1.14 ± 0.04	0.035	0.069 ± 0.035	0.069	3b	This study (excluding Sabrina Coast samples)
Uvigerina spp.	3	0.86 ± 0.03	0.035	0.070 ± 0.003	0.004	n/a	Elderfield et al., 2010 (and references therein)
Uvigerina spp. & *Trifarina angulosa*	4	0.97 ± 0.03	0.029	0.061 ± 0.003	0.061	4	Elderfield et al., 2010 & this study
Uvigerina spp. & *Trifarina angulosa*	5	0.98 ± 0.03	0.031	0.060 ± 0.003	0.003	4	Elderfield et al., 2010 & this study excluding Sabrina Coast
Bullimina spp.	6	0.94 ± 0.08	0.080	0.114 ± 0.011	0.011	n/a	Grunert et al., 2017
Bullimina spp.	7	1.04 ± 0.07	0.066	0.100 ± 0.010	0.010	5	Grunert et al., 2017 & this study
Globocassidulina spp.	8	0.99 ± 0.03	0.030	0.087 ± 0.009	0.001	6	Kristjánsdóttir et al., 2007; Tisserand et al., 2013; Barrientos et al., 2017 & this study

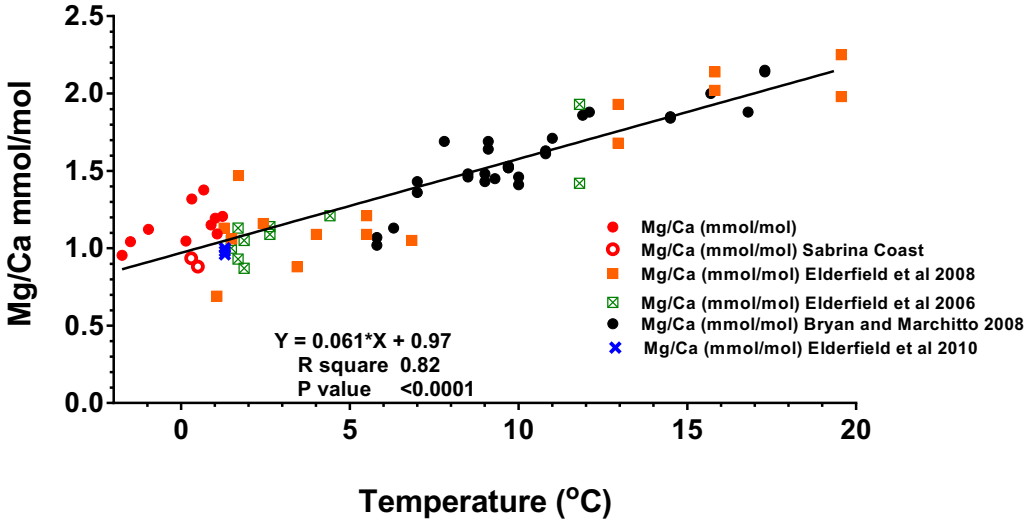

Fig. 4. Mg/Ca ratios versus temperature for *Trifarina angulosa* combined with published *Uvigerina* spp. Mg/Ca-BWT data. The published data obtained by oxidative cleaning adjusted by minus 0.2 mmol/mol. (Elderfield et al., 2010).

value of 0.42, indicating no correlation between Mg/Ca ratios and temperature. When plotted together with the data from the 250–355 μm fraction (Supplementary Fig. 3) no consistent offset in the Mg/Ca data is observed between the two size fractions.

3.2. *Bulimina aculeata* (250–355 μm)

Four surface sediment samples had a sufficient number of *Bulimina aculeata* tests for trace metal analysis, covering a small BWT range of +0.92 to +1.23℃ (Fig. 5). The addition of these data to a published *Bulimina* spp. calibration data set (Grunert et al., 2017, Equation 6) results in a minor change in the T-Mg/Ca slope and intercept (Equation 7; $R^2 = 0.64$, $P < 0.0001$).

3.3. *Globocassidulina subglobosa* (250–355 μm)

When plotted in isolation, the *Globocassidulina subglobosa* Mg/Ca data from our samples that span a narrow BWT range of −1.6 to +1.12℃ do not show a positive correlation with BWT ($R^2 = 0.02$, $P = 0.81$). However, when combined with published data for *Cassidulina subglobosa* (Tisserand et al., 2013) and *Cassidulina neoteretis* (Kristjánsdóttir et al., 2007; Barrientos et al., 2018) across

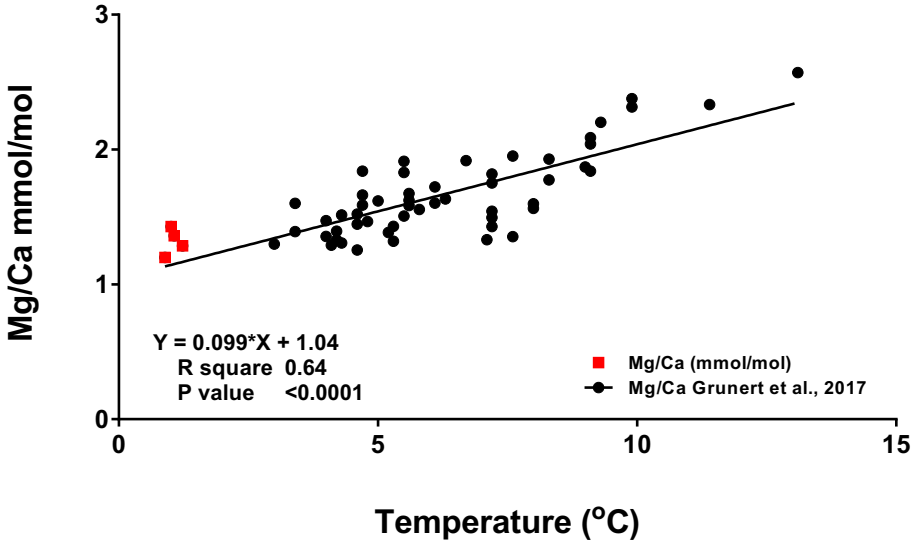

Fig. 5. Mg/Ca ratios versus temperature for *Bulimina aculeata* with published *Bulimina* spp. Mg/Ca-T data (from Grunert et al., 2018).

a broader BWT range, there is a linear fit ($R^2 = 0.71$, P=< 0.0001; Fig. 6, Equation 8).

4. DISCUSSION

4.1. *Trifarina angulosa*

The relationship between Mg/Ca ratios and BWT presented here for *Trifarina angulosa*, whilst positive and comparable to that seen in the published records of *Uvigerina* spp. (Elderfield et al., 2010 and references therein), shows large variability, which results in a relatively low R^2 value for the regression between Mg/Ca and BWT. We first consider the impact of different BWT calibrations on down-core data before discussing the limitations of our study and possible explanations for the scatter in our *Trifarina angulosa* data.

Because the gradient and intercept of the calibration equations vary, the various equations (Table 2, Equations 1–2, 4–5) result in relatively large differences between calculated temperature. This is demonstrated in Fig. 7, where Equations 1, 2 and 4 are applied to pilot down-core data from a core recovered from the outer western Amundsen Sea shelf (Smith et al., 2011). This offset is similar to the

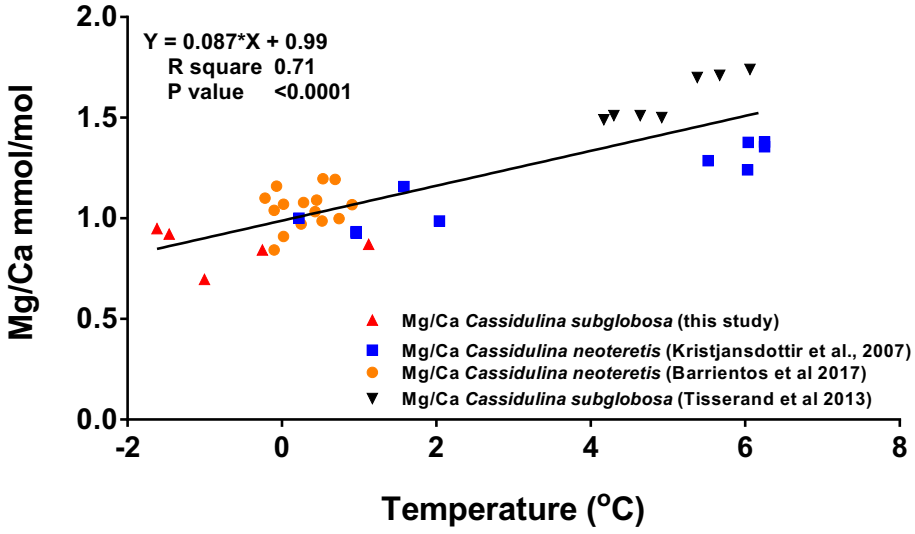

Fig. 6. Mg/Ca ratios versus temperature for *Cassidulina subglobosa* plotted with published Mg/Ca-BWT data for *Cassidulina subglobosa* and *Cassidulina neoteretis* (Kristjánsdóttir et al., 2007; Tisserand et al., 2013; Barrientos et al., 2018).

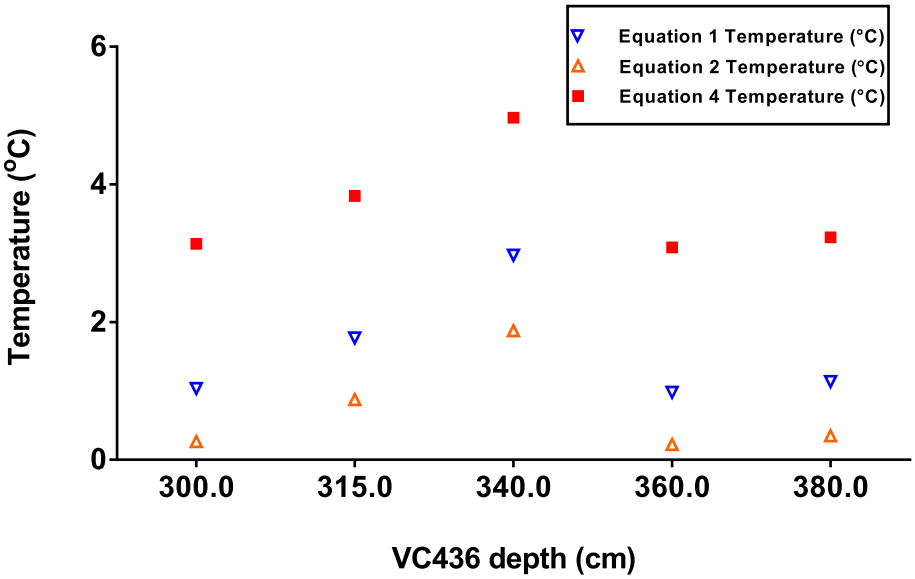

Fig. 7. Early Holocene BWTs derived from Mg/Ca ratios in *Trifarina angulosa* using equations 1, 2 and 4 (see text for details) Down-core samples are from core VC436 on the western Amundsen Sea shelf. The age range of the samples spans ~12.5 to 10.5 cal ka BP (Smith et al., 2011).

variability seen within the different datasets that comprise the most recently published *Uvigerina* spp. calibration (Elderfield et al., 2010). Whilst the various calibrations create large differences in reconstructed BWTs, the amplitude of down-core changes in BWT appears to be similar. Of the three calibrations used, Equation 2 produces BWTs (+0.2 to +1.8 °C) that are closest to the measured BWT range of seawater temperature in the Amundsen Sea (−1.5 to +1.4 °C; note that CDW has a temperature range of +0.2 to +1.4 °C). This might imply that regional calibrations offer the most promise in reconstructing palaeo BWTs. However, until these calibrations are applied to a wide range of down-core data, it remains unclear if this is the case for all sectors of the Antarctic continental margin.

One limitation of our study that cannot be easily overcome is the lack of modern *Trifarina angulosa* samples from Antarctic margin sites with a wide BWT range. This is partially related to a general lack of calcareous microfossils in modern sediments from the Antarctic continental margin, although further suitable locations (e.g., Hauck et al., 2012) may be (re-)sampled during future fieldwork campaigns. Furthermore, low concentration of calcareous microfossils often relates to sediment dilution, owing to the high-sedimentation rates in glaci-proximal settings. Targeting more distal settings with lower sedimentation rates, or shallower basins might increase the chances of finding microfossil-rich sediments in sufficient quantities to perform trace-metal geochemistry. Secondly, the ambient seawater temperature range for *Trifarina angulosa* around Antarctica is relatively narrow, so any regional core top calibration is inevitably constrained and cannot be as broad as that for *Uvigerina* spp. (Elderfield et al., 2010). Laboratory cultures of benthic foraminifera are challenging, and calibrations based on cultured specimens of *Trifarina angulosa* grown under conditions outside of their natural temperature range may result in BWT-Mg/Ca relationships that are not applicable to down-core material.

Environmental variables, such as carbonate saturation state (Elderfield et al., 2006, Bryan and Marchitto, 2008), and the Mg/Ca content of seawater (Evans and Müller, 2012) may exert secondary influences on the Mg/Ca ratio of foraminifera shells. However, Mg/Ca ratios of shallow infaunal species, such as *Uvigerina* spp., *Trifarina angulosa,* and *Oridorsalis umbonatus*, are generally considered less sensitive to changes in the bottom water carbonate saturation state than those of epifaunal species (Elderfield et al., 2010, Brown et al., 2011, Mawbey and Lear, 2013) as they inhabit sediments with pore-waters that are thought to equilibrate rapidly with calcium carbonate (Elderfield et al., 2006). This notwithstanding, it has been observed for the species *Oridorsalis umbonatus* that large changes in carbonate saturation state in seawater may penetrate the sediments, creating so called "dissolution events" that could affect the Mg/Ca ratios in shallow infaunal foraminifera shells (Mawbey and Lear, 2013). Furthermore, measurements of pore-water carbonate saturation state revealed its spatial variability, and a relationship between pore-water and bottom water carbonate ion saturation state (Weldeab et al., 2016). Therefore, Mg/Ca data from regions that may be subject to large changes in carbonate saturation state, such as those episodically or periodically bathed by relatively unmodified CDW, should be treated with caution. B/Ca is a possible proxy for carbonate ion saturation state (Rae et al., 2011) and was measured on the samples of this study (Supplementary Figs. 4 and 5). However, the B/Ca ratios of *Trifarina angulosa* were very low (~10 μmmol/mol) and, compared to the analytical blank (~10 μmol/mol vs. ~2 μmol/mol), not analytically robust enough for an interpretation (cf. Hillenbrand et al., 2017). The measured low B/Ca ratios are consistent with those of *Uvigerina* sp. (Doss et al., 2018), and other shallow infaunal species, such as *Oridorsalis umbonatus* (Brown et al., 2011).

Seawater Mg/Ca ratios (Mg/Ca_{sw}) are generally thought to have a potential influence on Mg/Ca ratios in foraminifera (Evans et al., 2012). The long residence times of Mg and Ca in the oceans (~14 Myr and ~1 Myr, respectively (Evans et al., 2012)) imply that global changes in Mg/Ca_{sw} only become significant over long timescales and are therefore of negligible importance to our surface sediment study. However, some of the sample sites in our study are relatively shallow (Table 1) and are perhaps subject to changes in Mg/Ca_{sw} on a local scale, which might have caused the variability of Mg/Ca in foraminiferal calcite observed by us. Localised seawater chemistry variability could be excluded as a driving mechanism for foraminiferal Mg/Ca in a future study through trace metal measurements on seawater samples and foraminifera shells from sediment samples collected at the same sites. Work by Lear et al. (2015) on the shallow infaunal benthic foraminifera species *Oridorsalis umbonatus* suggests that its Mg/Ca ratio is only weakly affected by Mg/Ca_{sw} due to the foraminiferal biological regulation of Mg/Ca uptake. It is plausible that this is the case for other benthic foraminifera species, too, which would limit the effect of Mg/Ca_{sw} on the measured Mg/Ca values. This warrants investigation and could influence the choice of species selected to evaluate Mg/Ca in foraminifera from around the Antarctic continental margin.

Finally, it has been previously demonstrated that shell size can have an important influence on stable carbon and oxygen isotope (Birch et al., 2013) and trace metal composition (Friedrich et al., 2012) of planktic foraminifera. The effect of test size on trace metal concentrations in benthic foraminifera is also possible, although less well understood (Franco-Fraguas et al., 2011, Diz et al., 2012, and Hintz et al., 2006). A potential size effect is supported by our data because the 150–250 μm Mg/Ca ratios of *Trifarina anguolsa* do not show a correlation with BWT (Supplementary Fig. 2). To mitigate this potential effect, we recommend using a larger size fraction. In our study, we could compare Mg/Ca data for 10 out of 12 samples, which had enough specimens in both the 150–250 μm and the 250–355 μm size fractions. From the remaining two samples (MC45 and MC61 from the Sabrina Coast), we had to analyse tests from the 150–355 μm fraction. These two samples are excluded from the final calibration (Fig. 3b), Table 2 equation 2, as they fall outside the 95% confidence interval of the calibration. The equation including the Sabrina Coast samples (Fig. 3a, Equation 1) is however included in Table 2. These two samples included the "Hispid" (spiky) morpho-

type of *Trifarina angulosa*, whereas our other samples contained exclusively the Costate (ribbed) morphotype. Investigation into whether an offset between these two morphotypes exists will be possible in the future, when more samples become available, which might improve the Mg/Ca-BWT calibration.

4.2. *Bulimina aculeata*

The addition of new *Bulimina aculeata* Mg/Ca-BWT data to the calibration of Grunert et al. (2018) neither reduces the Mg/Ca-BWT relationship ($R^2 = 0.64$ in both instances) nor modifies the existing calibration significantly (Table 2, Equations 6 to 7). With an Mg/Ca value of 1.0 mmol/mol, use of the two equations results in a BWT difference of only 0.1 °C. This finding supports the conclusion that this calibration may be used across different species of *Bulimina* spp. and can be extended to BWTs of ≤ 3 °C.

4.3. *Globocassidulina* spp.

The combined Mg-Ca BWT data sets for *Globocassidulina* spp. from this study and previously published studies (Kristjánsdóttir et al., 2007; Tisserand et al., 2013; Barrientos et al., 2018) indicate a robust positive relationship between Mg/Ca and BWT. As with the other two species presented herein, the variability within the dataset does indicate that factors other than BWT and analytical error may influence foraminiferal Mg/Ca ratios.

5. CONCLUSIONS

The aim of this study was to investigate the applicability of Mg/Ca benthic foraminiferal palaeothermometry to the climatically sensitive continental shelf of Antarctica. Of the three different species/genera studied *Bulimina aculeata* has the highest Mg/Ca sensitivity to BWT, followed by *Globocassidulina* spp. *Trifarina angulosa* also displays a positive relationship with temperature, but is less sensitive than the other two species. In this respect, it is advantageous to have multiple calibrations available in the paleothermometry toolkit as the availability of species varies across different oceanographic and environmental settings. This is particularly pertinent to Antarctic shelf areas where preservation of calcareous foraminifera is patchy at best.

The positive correlations between Mg/Ca ratios of the studied benthic foraminifera shells and BWT, whilst indicative of a strong relationship between the two, show considerable variance. Such variability indicates that Mg/Ca ratios in these foraminifera species may also depend upon other environmental parameters, which have not been evaluated in this study. Sampling of seafloor surface sediment and bottom (and pore-) water samples from the same sites and combined (geo-) chemical measurements on these samples are the next step forward in unravelling the role of these other factors. Mg/Ca-BWT calibrations, such as those produced here, require cautious use, demand further ground-truthing through application to down-core records, and should be used in conjunction with other proxies, such as those for seawater temperature, alkalinity and salinity. Furthermore, additional studies are required to determine if regional-only or global calibration datasets are most appropriate for down-core studies. For *Trifarina angulosa*, we observe that our regional calibration produces BWTs that are most comparable to measured seawater temperatures in the Amundsen Sea.

Declaration of Competing Interest

The authors declare that they have no known competing financial interests or personal relationships that could have appeared to influence the work reported in this paper.

ACKNOWLEDGEMENTS

We thank the captain, crew, shipboard scientists and support staff participating in RRS *James Clark Ross* expeditions JR104 and JR141, RV *Polarstern* expeditions ANT-II/3, ANT-1V/3, ANT-VI/2, ANT-IX/3 and ANT-XXIII/4 and RV/IB *Nathaniel B. Palmer* expedition NBP14-02. Furthermore, we are grateful to Prof. Andreas Mackensen (AWI) for providing picked foraminifera samples. This study was funded by the Natural Environment Research Council grant NE/M013081/1, awarded to J.A.S., K.H. H., E.L.M and C.D.H. Additional funding from grants NE/M013782/1, NE/M013243/1 and NSF Antarctic Integrated Systems Science Program #1143834, 1143836, 1143837, 1143843, and 1313826 and NSF Antarctic Earth Sciences #1744970 to A.E.S is also acknowledged. Finally we thank two anonymous reviewers and the editorial guidance of Dr. Tom Marchitto which helped improve our manuscript.

APPENDIX A. SUPPLEMENTARY DATA

Supplementary data to this article can be found online at https://doi.org/10.1016/j.gca.2020.05.027.

REFERENCES

Barker S., Greaves M. and Elderfield H. (2003) A study of cleaning procedures used for foraminiferal Mg/Ca paleothermometry. *Geochem. Geophys. Geosyst.* **4**(9), 8407. https://doi.org/10.1029/2003GC000559.

Barrientos N., Lear C. H., Jakobsson M., Stranne C., O'Regan M., Cronin T. M., Gukov A. Y. and Coxall H. K. (2018) Arctic Ocean benthic foraminifera Mg/Ca ratios and global Mg/Ca-temperature calibrations: New constraints at low temperatures. *Geochim. Cosmochim. Acta* **236**, 240–259. https://doi.org/10.1016/j.gca.2018.02.036.

Birch H., Coxall H. K., Pearson P. N., Kroon D. and O'Regan M. (2013) Planktonic foraminifera stable isotopes and water column structure: Disentangling ecological signals. *Mar. Micropaleontol.* **101**, 127–145. https://doi.org/10.1016/j.marmicro.2013.02.002.

Boyle E. and Keigwin L. (1985) Comparison of Atlantic and Pacific paleochemical records for the last 215,000 years: Changes in deep ocean circulation and chemical inventories. *Earth Planet. Sci. Lett.* **76**, 135–150.

Brown R. E., Anderson L. D., Thomas E. and Zachos J. C. (2011) A core-top calibration of B/Ca in the benthic foraminifers Nuttallides umbonifera and Oridorsalis umbonatus: A proxy for Cenozoic bottom water carbonate saturation. *Earth Planet.*

Sci. Lett. **310**, 360–368. https://doi.org/10.1016/j.epsl.2011.08.023.

Bryan S. P. and Marchitto T. M. (2008) Mg/Ca–temperature proxy in benthic foraminifera: New calibrations from the Florida Straits and a hypothesis regarding Mg/Li. *Paleoceanography and Paleoclimatology* **23**. https://doi.org/10.1029/2007PA001553.

Colleoni F., De Santis L., Siddoway C. S., Bergamasco A., Golledge N. R., Lohmann G., Passchier S. and Siegert M. J. (2018) Spatio-temporal variability of processes across Antarctic ice-bed–ocean interfaces. *Nat. Commun.* **9**, 2289. https://doi.org/10.1038/s41467-018-04583-0.

de Villiers S., Greaves M. and Elderfield H. (2002) An intensity ratio calibration method for the accurate determination of Mg/Ca and Sr/Ca of marine carbonates by ICP-AES. *Geochem. Geophys. Geosyst.* **3**, 623–634. https://doi.org/10.1029/2001GC000169.

DeConto R. M. and Pollard D. (2016) Contribution of Antarctica to past and future sea-level rise. *Nature* **531**, 591. https://doi.org/10.1038/nature17145.

Diz P., Barras C., Geslin E., Reichart G.-J., Metzger E., Jorissen F. and Bijma J. (2012) Incorporation of Mg and Sr and oxygen and carbon stable isotope fractionation in cultured Ammonia tepida. *Mar. Micropaleontol.* **92**, 16–28. https://doi.org/10.1016/j.marmicro.2012.04.006.

Doss W., Marchitto T. M., Eagle R., Rashid H. and Tripati A. (2018) Deconvolving the saturation state and temperature controls on benthic foraminiferal Li/Ca, based on downcore paired B/Ca measurements and coretop compilation. *Geochim. Cosmochim. Acta* **236**, 297–314. https://doi.org/10.1016/j.gca.2018.02.029.

Dutrieux P., De Rydt J., Jenkins A., Holland P. R., Ha H. K., Lee S. H., Steig E. J., Ding Q., Abrahamsen E. P. and Schröder M. (2014) Strong sensitivity of Pine Island ice-shelf melting to climatic variability. *Science* **343**, 174–178. https://doi.org/10.1126/science.1244341.

Edwards T. L., Brandon M. A., Durand G., Edwards N. R., Golledge N. R., Holden P. B., Nias I. J., Payne A. J., Ritz C. and Wernecke A. (2019) Revisiting Antarctic ice loss due to marine ice-cliff instability. *Nature* **566**, 58–64. https://doi.org/10.1038/s41586-019-0901-4.

Elderfield H., Greaves M., Barker S., Hall I. R., Tripati A., Ferretti P., Crowhurst S., Booth L. and Daunt C. (2010) A record of bottom water temperature and seawater δ 18 O for the Southern Ocean over the past 440kyr based on Mg/Ca of benthic foraminiferal Uvigerina spp. *Quat. Sci. Rev.* **29**, 160–169. https://doi.org/10.1016/j.quascirev.2009.07.013.

Elderfield H., Yu J., Anand P., Kiefer T. and Nyland B. (2006) Calibrations for benthic foraminiferal Mg/Ca paleothermometry and the carbonate ion hypothesis. *Earth Planet. Sci. Lett.* **250**, 633–649. https://doi.org/10.1016/j.epsl.2006.07.041.

Etourneau J., Collins L. G., Willmott V., Kim J.-H., Barbara L., Leventer A., Schouten S., Damsté J. S., Bianchini A. and Klein V. (2013) Holocene climate variations in the western Antarctic Peninsula: evidence for sea ice extent predominantly controlled by changes in insolation and ENSO variability. *Clim. Past* **9**, 1431–1446. https://doi.org/10.5194/cp-9-1431-2013.

Evans D., Erez J., Oron S. and Müller W. (2015) Mg/Ca-temperature and seawater-test chemistry relationships in the shallow-dwelling large benthic foraminifera Operculina ammonoides. *Geochim. Cosmochim. Acta* **148**, 325–342. https://doi.org/10.1002/2014PA002735.

Evans D. and Müller W. (2012) Deep time foraminifera Mg/Ca paleothermometry: Nonlinear correction for secular change in seawater Mg/Ca. *Paleoceanography* **27**. https://doi.org/10.1029/2012PA002315.

Franco-Fraguas P., Costa K. B. and Toledo F. A. D. L. (2011) Stable isotope/test size relationship in Cibicidoides wuellerstorfi. *Braz. J. Oceanogr.* **59**, 287–291. https://doi.org/10.1590/S1679-87592011000300010.

Friedrich O., Schiebel R., Wilson P. A., Weldeab S., Beer C. J., Cooper M. J. and Fiebig J. (2012) Influence of test size, water depth, and ecology on Mg/Ca, Sr/Ca, δ18O and δ13C in nine modern species of planktic foraminifers. *Earth Planet. Sci. Lett.* **319**, 133–145. https://doi.org/10.1016/j.epsl.2011.12.002.

Greaves M., Caillon N., Rebaubier H., Bartoli G., Bohaty S., Cacho I., Clarke L., Cooper M., Daunt C. and Delaney M. (2008) Interlaboratory comparison study of calibration standards for foraminiferal Mg/Ca thermometry. *Geochem. Geophys. Geosyst.* **9**, Q08010. https://doi.org/10.1029/2008GC001974.

Grunert P., Rosenthal Y., Jorissen F., Holbourn A., Zhou X. and Piller W. E. (2018) Mg/Ca-temperature calibration for costate Bulimina species (B. costata, B. inflata, B. mexicana): A paleothermometer for hypoxic environments. *Geochim. Cosmochim. Acta* **220**, 36–54. https://doi.org/10.1016/j.gca.2017.09.021.

Hauck J., Gerdes D., Hillenbrand C.-D., Hoppema M., Kuhn G., Nehrke G., Völker C. and Wolf-Gladrow D. A. (2012) Distribution and mineralogy of carbonate sediments on Antarctic shelves. *J. Mar. Syst.* **90**, 77–87. https://doi.org/10.1016/j.jmarsys.2011.09.005.

Hillenbrand C.-D., Smith J. A., Hodell D. A., Greaves M., Poole C. R., Kender S., Williams M., Andersen T. J., Jernas P. E., Elderfield H., Klages J. P., Roberts S. J., Gohl K., Larter R. D. and Kuhn G. (2017) West Antarctic Ice Sheet retreat driven by Holocene warm water incursions. *Nature* **547**, 43–48. https://doi.org/10.1038/nature22995.

Hintz C. J., Shaw T. J., Bernhard J. M., Chandler G. T., McCorkle D. C. and Blanks J. K. (2006) Trace/minor element: calcium ratios in cultured benthic foraminifera. Part II: Ontogenetic variation. *Geochim. Cosmochim. Acta* **70**, 1964–1976. https://doi.org/10.1016/j.gca.2005.12.019.

Holland P, Bracegirdle T. J., Dutrieux P., Jenkins A. and Steig E. J. (2019) West Antarctic ice loss influenced by internal climate variability and anthropogenic forcing. *Nat. Geosci.* **12**, 718–724. https://doi.org/10.1038/s41561-019-0420-9.

Ishman S. E. (1990) *Quantitative analysis of Antarctic benthic foraminifera: Application to paleoenvironmental interpretations*. State University, The Ohio.

Ishman S. E. and Domack E. W. (1994) Oceanographic controls on benthic foraminifers from the Bellingshausen margin of the Antarctic Peninsula. *Mar. Micropaleontol.* **24**, 119–155. https://doi.org/10.1016/0377-8398(94)90019-1.

Jacobs S., Jenkins A., Giulivi C. F. and Dutrieux P. (2011) Stronger ocean circulation and increased melting under Pine Island Glacier ice shelf. *Nat. Geosci.* **4**, 519–523. https://doi.org/10.1038/NGEO1188.

Jenkins A., Shoosmith D., Dutrieux P., Jacobs S., Kim T. W., Lee S. H., Ha H. K. and Stammerjohn S. (2018) West Antarctic Ice Sheet retreat in the Amundsen Sea driven by decadal oceanic variability. *Nat. Geosci.* **11**, 733–738. https://doi.org/10.1038/s41561-018-0207-4.

Kim J. H., Crosta X., Willmott V., Renssen H., Bonnin J., Helmke P., Schouten S. and Sinninghe Damsté J. S. (2012) Holocene subsurface temperature variability in the eastern Antarctic continental margin. *Geophys. Res. Lett.* **39**, L06705. https://doi.org/10.1029/2012GL051157.

Kristjánsdóttir G. B., Lea D. W., Jennings A. E., Pak D. K. and Belanger C. (2007) New spatial Mg/Ca-temperature calibrations for three Arctic, benthic foraminifera and reconstruction of north Iceland shelf temperature for the past 4000 years: Mg/

Ca-TEMPERATURE CALIBRATIONS. *Geochem. Geophys. Geosyst.* **8**(3), n/a–n/a. https://doi.org/10.1029/2006GC001425.

Lear C. H., Coxall H. K., Foster G. L., Lunt D. J., Mawbey E. M., Rosenthal Y., Sosdian S. M., Thomas E. and Wilson P. A. (2015) Neogene ice volume and ocean temperatures: Insights from infaunal foraminiferal Mg/Ca paleothermometry. *Paleoceanography* **30**, 1437–1454. https://doi.org/10.1002/2015PA002833.

Leventer A., Domack E., Barkoukis A., McAndrews B. and Murray J. (2002) Laminations from the Palmer Deep: A diatom-based interpretation. *Paleoceanogr. Paleoclimatol.* **17** (2), 8002. https://doi.org/10.1029/2001PA000624.

Mackensen A., Grobe H., Kuhn G. and Fütterer D. K. (1990) Benthic foraminiferal assemblages from the eastern Weddell Sea between 68 and 73°S: Distribution, ecology and fossilization potential. *Mar. Micropaleontol.* **16**, 241–283.

Mackensen A., Hubberten H.-W., Bickert T., Fischer G. and Fütterer D. K. (1993) The $\delta^{13}C$ in benthic foraminiferal tests of Fontbotia wuellerstorfi (Schwager) Relative to the $\delta^{13}C$ of dissolved inorganic carbon in Southern Ocean deep water: implications for Glacial Ocean Circulation models. *Paleoceanography* **8**, 587–610.

Majewski W. (2013) Benthic foraminifera from Pine island and Ferrero bays, Amundsen sea. *Polish Polar Res.* **34**, 169–200. https://doi.org/10.2478/popore−2013−0012.

Majewski W. and Anderson J. B. (2009) Holocene foraminiferal assemblages from Firth of Tay, Antarctic Peninsula: paleoclimate implications. *Mar. Micropaleontol.* **73**, 135–147. https://doi.org/10.1016/j.marmicro.2009.08.003.

Majewski W. and Pawlowski J. (2010) Morphologic and molecular diversity of the foraminiferal genus Globocassidulina in Admiralty Bay, King George Island. *Antarct. Sci.* **22**, 271–281. https://doi.org/10.1017/S0954102010000106.

Majewski W., Tatur A., Witkowski J. and Gaździcki A. (2017) Rich shallow-water benthic ecosystem in Late Miocene East Antarctica (Fisher Bench Fm, Prince Charles Mountains). *Mar. Micropaleontol.* **133**, 40–49. https://doi.org/10.1016/j.marmicro.2017.06.002.

Marchitto T., Bryan S., Curry W. and McCorkle D. (2007) Mg/Ca temperature calibration for the benthic foraminifer Cibicidoides pachyderma. Paleoceanography and. *Paleoclimatology* **22**, PA1203. https://doi.org/10.1029/2006PA001287.

Mawbey E. M. and Lear C. H. (2013) Carbon cycle feedbacks during the Oligocene-Miocene transient glaciation. *Geology* **41**, 963–966. https://doi.org/10.1130/G34422.1.

Meredith M. P., Brandon M. A., Wallace M. I., Clarke A., Leng M. J., Renfrew I. A., Van Lipzig N. P. and King J. C. (2008) Variability in the freshwater balance of northern Marguerite Bay, Antarctic Peninsula: results from δ18O. *Deep Sea Res. Part II* **55**, 309–322. https://doi.org/10.1016/j.dsr2.2007.11.005.

Minzoni R. T., Majewski W., Anderson J. B., Yokoyama Y., Fernandez R. and Jakobsson M. (2017) Oceanographic influences on the stability of the Cosgrove Ice Shelf, Antarctica. *The Holocene* **27**, 1645–1658. https://doi.org/10.1177/0959683617702226.

Misra S., Greaves M., Owen R., Kerr J., Elmore A. C. and Elderfield H. (2014) Determination of B/Ca of natural carbonates by HR-ICP-MS. *Geochem. Geophys. Geosyst.* **15**, 1617–1628. https://doi.org/10.1002/2013GC005049.

Murray J. W. and Pudsey C. J. (2004) Living (stained) and dead foraminifera from the newly ice-free Larsen Ice Shelf, Weddell Sea, Antarctica: ecology and taphonomy. *Mar. Micropaleontol.* **53**, 67–81. https://doi.org/10.1016/j.marmicro.2004.04.001.

Peck V. L., Allen C. S., Kender S., McClymont E. L. and Hodgson D. A. (2015) Oceanographic variability on the West Antarctic Peninsula during the Holocene and the influence of upper circumpolar deep water. *Quaternary Science Reviews* **119**, 54–65. https://doi.org/10.1016/j.quascirev.2015.04.002.

Pritchard H., Ligtenberg S., Fricker H., Vaughan D., Van den Broeke M. and Padman L. (2012) Antarctic ice-sheet loss driven by basal melting of ice shelves. *Nature* **484**, 502–505. https://doi.org/10.1038/nature10968.

Rae J. W., Foster G. L., Schmidt D. N. and Elliott T. (2011) Boron isotopes and B/Ca in benthic foraminifera: Proxies for the deep ocean carbonate system. *Earth Planet. Sci. Lett.* **302**, 403–413. https://doi.org/10.1016/j.epsl.2010.12.034.

Rathburn A. E. and De Deckker P. (1997) Magnesium and strontium compositions of recent benthic foraminifera from the Coral Sea, Australia and Prydz Bay, Antarctica. *Mar. Micropaleontol.* **32**, 231–248. https://doi.org/10.1016/S0377-8398(97)00028-5.

Rignot E., Mouginot J., Scheuchl B., van den Broeke M., van Wessem M. J. and Morlighem M. (2019) Four decades of Antarctic Ice Sheet mass balance from 1979–2017. In *Proceedings of the National Academy of Sciences*, pp. 1095–1103. https://doi.org/10.1073/pnas.1812883116.

Rosenthal Y., Boyle E. A. and Slowey N. (1997) Temperature control on the incorporation of magnesium, strontium, fluorine, and cadmium into benthic foraminiferal shells from Little Bahama Bank: Prospects for thermocline paleoceanography. *Geochim. Cosmochim. Acta* **61**, 3633–3643. https://doi.org/10.1016/S0016-7037(97)00181-6.

Rosenthal Y., Perron-Cashman S., Lear C. H., Bard E., Barker S., Billups K., Bryan M., Delaney M. L., Demenocal P. B. and Dwyer G. S. (2004) Interlaboratory comparison study of Mg/Ca and Sr/Ca measurements in planktonic foraminifera for paleoceanographic research. *Geochem. Geophys. Geosyst.* **5**, 4. https://doi.org/10.1029/2003GC000650.

Schmidtko S., Heywood K. J., Thompson A. F. and Aoki S. (2014) Multidecadal warming of Antarctic waters. *Science* **346**, 1227–1231. https://doi.org/10.1126/science.1256117.

Schweizer M., Pawlowski J., Duijnstee I. A. P., Kouwenhoven T. J. and van der Zwaan G. J. (2005) Molecular phylogeny of the foraminiferal genus Uvigerina based on ribosomal DNA sequences. *Mar. Micropaleontol.* **57**(3–4), 51–67. https://doi.org/10.1016/j.marmicro.2005.07.001.

Schweizer M., Jorissen F. and Geslin E. (2011) Contributions of molecular phylogenetics to foraminiferal taxonomy: general overview and example of Pseudoeponides falsobeccarii. *C.R. Palevol* **10**, 95–105. https://doi.org/10.1016/j.crpv.2011.01.003.

Shackleton N. (1967) Oxygen isotope analyses and Pleistocene temperatures re-assessed. *Nature* **215**, 15–17.

Shevenell A., Ingalls A., Domack E. and Kelly C. (2011) Holocene Southern Ocean surface temperature variability west of the Antarctic Peninsula. *Nature* **470**, 250–254. https://doi.org/10.1038/nature09751.

Shevenell A. E. and Kennett J. P. (2002) Antarctic Holocene climate change: A benthic foraminiferal stable isotope record from Palmer Deep. *Paleoceanography* **17**, 2. https://doi.org/10.1029/2000PA000596.

Skirbekk K., Hald M., Marchitto T. M., Junttila J., Kristensen D. K. and Sørensen S. A. (2016) Benthic foraminiferal growth seasons implied from Mg/Ca-temperature correlations for three Arctic species. *Geochem. Geophys. Geosyst.* **17**, 4684–4704. https://doi.org/10.1002/2016GC006505.

Smith J., Andersen T. J., Shortt M., Gaffney A., Truffer M., Stanton T., Bindschadler R., Dutrieux P., Jenkins A. and Hillenbrand C.-D. (2017) Sub-ice-shelf sediments record history of twentieth-century retreat of Pine Island Glacier. *Nature* **541**, 77. https://doi.org/10.1038/nature20136.

Smith J. A., Hillenbrand C.-D., Kuhn G., Larter R. D., Graham A. G., Ehrmann W., Moreton S. G. and Forwick M. (2011)

Deglacial history of the West Antarctic Ice Sheet in the western Amundsen Sea embayment. *Quat. Sci. Rev.* **30**, 488–505. https://doi.org/10.1016/j.quascirev.2010.11.020.

Steig E. J., Ding Q., Battisti D. and Jenkins A. (2012) Tropical forcing of Circumpolar Deep Water inflow and outlet glacier thinning in the Amundsen Sea Embayment, West Antarctica. *Ann. Glaciol.* **53**, 19–28. https://doi.org/10.3189/2012AoG60A110.

Tisserand A. A., Dokken T. M., Waelbroeck C., Gherardi J. M., Scao V., Fontanier C. and Jorissen F. (2013) Refining benthic foraminiferal Mg/Ca-temperature calibrations using core-tops from the western tropical Atlantic: Implication for paleotemperature estimation. *Geochem. Geophys. Geosyst.* **14**, 929–946. https://doi.org/10.1002/ggge.20043.

Vaughan D. G., Corr H. F., Ferraccioli F., Frearson N., O'Hare A., Mach D., Holt J. W., Blankenship D. D., Morse D. L. and Young D. A. (2006) New boundary conditions for the West Antarctic ice sheet: Subglacial topography beneath Pine Island Glacier. *Geophys. Res. Lett.* **33**. https://doi.org/10.1029/2005GL025588.

Weldeab S., Arce A. and Kasten S. (2016) Mg/Ca-$\Delta CO_{3\ pore\ water}^{2-}$-temperature calibration for Globobulimina spp.: A sensitive paleothermometer for deep-sea temperature reconstruction. *Earth Planet. Sci. Lett.* **438**, 95–102. https://doi.org/10.1016/j.epsl.2016.01.009.

Associate editor: Thomas M. Marchitto